

## 3-[[3-(Triethoxysilyl)-propyl] amino] propane-1-sulfonic acid zwitterion grafted polyvinylidene fluoride antifouling membranes for concentrating greywater in direct contact membrane distillation

Jin Wang<sup>a,b</sup>, Hailong He<sup>c</sup>, Mengliang Wang<sup>a,c</sup>, Zechun Xiao<sup>a,b</sup>, Ying Chen<sup>a</sup>, Yanqiang Wang<sup>d</sup>, Jianfeng Song<sup>a,b</sup>, Xue-Mei Li<sup>a</sup>, Yuebiao Zhang<sup>c</sup>, Tao He<sup>a,c,\*</sup>

<sup>a</sup> Shanghai Advanced Research Institute, Chinese Academy of Sciences, Shanghai 201210, China

<sup>b</sup> University of Chinese Academy of Sciences, Beijing 100049, China

<sup>c</sup> School of Physical Science and Technology, ShanghaiTech University, Shanghai 201210, China

<sup>d</sup> Disney Research Center China, Shanghai 200031, China

### ARTICLE INFO

#### Keywords:

Hydrophilic-hydrophobic  
Grey water  
Membrane distillation  
Anti-fouling, zwitterionic

### ABSTRACT

Direct contact membrane distillation (DCMD) is attractive for wastewater reuse where low-grade heat is highly abundant, but membrane fouling is of critical concerns. In this work, a zwitterion surface-grafted composite polyvinylidene fluoride membrane (PVDF-T) was introduced for DCMD treatment of greywater, a lightly polluted wastewater. Surface grafting was achieved by hydroxylation of a pristine PVDF membrane followed by silanization with the zwitterionomer 3-[[3-(triethoxysilyl)-propyl] amino] propane-1-sulfonic acid (TPAPS). The resulting composite PVDF-T membrane showed a significantly reduced water contact angle but nearly the same liquid entry pressure (LEP) indicating that silanization took place mostly at the surface, and the porous matrix remained hydrophobic. Elemental analysis confirmed that the TPAPS surface grafting was successful. Gas permeability tests indicated increased transport resistance, indicating the extra resistance imposed the zwitterionic modification. In concentrating the synthetic greywater, the PVDF-T membrane exhibited much more stable DCMD flux and constant permeate conductivity than the virgin PVDF membrane. Visual and scanning electron microscopy analysis after MD experiments showed that the PVDF-T membrane was fouled less than the pristine membrane. Improvement in surface hydrophilicity, electronegative charge and steric hindrance were ascribed as the main factors for the fouling resistance of a surface grafted zwitterionic composite PVDF membrane.

### 1. Introduction

Energy-water nexus is a key contemporary focus of the global challenges [1]. The treatment of municipal wastewater is usually achieved through biological treatment via aerobic digestion, which is energy intensive with a large footprint [2,3]. The waste streams from households can be differentiated into greywater, produced from bathtubs, showers, hand basins, laundry machines and kitchen sinks [4], and black water [4,5], produced from the toilets. Because greywater contains much less organic content than the black water, separate treatment of greywater will greatly reduce the wastewater volume needed for biological treatment. Another advantage of the separate treatment is that the biological oxygen demand (BOD) of wastewater can be maintained at a more stable level and therefore, the maintenance of a wastewater treatment plant will be less demanding. Greywater can

be treated using advanced desalination membrane processes including reverse osmosis, nanofiltration and FO [6,7]. One common issue in utilizing membrane treatment is membrane fouling. Still more challenging for membrane distillation treatment of greywater is membrane wetting because of the presence of surfactants.

In this paper, we will address the use of membrane distillation in a broader concept for smart city design combining both water and energy factors [8,9]. The case is located at the Shanghai Disneyland resort, which is retrofitted with a thermal power plant generating a large amount of waste heat. At the same time, the resort requires clean water free of organic and inorganic contaminants for recreation purposes. The concept of the project is to utilize the waste heat for the MD process to recycle the greywater from the resort [10,11]. The MD process produces in principal nearly pure water which can be fed back to the existing water circles in the resort. Because of the low foulant content in

\* Corresponding author at: Shanghai Advanced Research Institute, Chinese Academy of Sciences, Shanghai 201210, China.

E-mail address: [het@sari.ac.cn](mailto:het@sari.ac.cn) (T. He).

<https://doi.org/10.1016/j.desal.2019.01.009>

Received 13 December 2018; Received in revised form 9 January 2019; Accepted 9 January 2019

0011-9164/ © 2019 Elsevier B.V. All rights reserved.

the feed, very high water recovery is expected; the concentrate containing high organic concentrate can be directed to the conventional wastewater treatment plant; a compact system would reduce the footprint and leave space for the commercial purpose. However, the fouling and performance of hydrophobic membrane in treating greywater is largely unknown.

Since salinity of the greywater is low, inorganic fouling or scaling in MD is not a major concern [12,13]. However, organics, soluble or insoluble, exist in a wide spectrum: caseins from milk products, surfactants from detergents and humic matters adsorbed to mineral surfaces [14,15]. For organic fouling, the hydrophobic interaction tends to drive the accumulation of foulants onto the hydrophobic membrane surface, or inside the pores [16]. The amphiphilic surfactants containing detergents [17,18] tend to foul the membrane and/or cause membrane wetting [19]. To obtain a high water recovery rate, it is highly important that the membrane organic fouling can be mitigated through an engineered approach.

Pre-treatment is the most efficient method to remove the organic foulants from the feed [11]. This will alleviate the stress of fouling for the hydrophobic membrane. Other approaches are focused on membranes. For example, superhydrophobic membranes have been reported for fouling reduction [20,21]. Omniphobic membranes have demonstrated resistance toward surfactants-induced wetting owing to the re-entrant structure [17,22], yet still suffered from oil fouling [23]. Enlightened by “Janus” structure, hydrophilic-hydrophobic composite membranes with a hydrophilic section outperformed superhydrophobic and omniphobic membranes both in terms of wetting and oil fouling resistance [23–25]. A hydrophilic layer has been introduced by various methods such as plasma grafting of polyethylene glycol and TiO<sub>2</sub> [25], dip-coating polydopamine/polyethyleneimine onto the hydrophobic polypropylene hollow fiber support [26], and chitosan and silica nanoparticle modified fiber layer onto a omniphobic substrate [19]. In principle, a thin controllable hydrophilic layer is sufficient to demonstrate antifouling property; only a hydrophilic layer is less efficient than a zwitterionic surface in fouling resistance [27]. It is anticipated that a very thin zwitterionic surface coating would show strong fouling resistance; however, to the author's knowledge, ionic coating layers, e.g. zwitterions, have not been tested yet.

Zwitterionic grafting has been widely practiced for the surface modification of hydrophilic membranes [28–30]. Beside the advantages of steric effect similar to other hydrophilic coating chemicals, the strong charge effect of zwitterions induced lower hydration free energy than nonionic moieties, thus less favorable for pollutants to intimately contact with membrane surface; the more hydration water molecule contributes to fouling resistance as well [31]. As for hydrophobic membranes, zwitterionic effects have not yet been reported on the wetting and antifouling properties of the MD membranes, neither for treatment of greywater. Aiming at stable coating, chemical bonding between the hydrophobic supports with strongly hydrophilic zwitterionic chemicals is crucial. Among different types of zwitterionic polymers [27,32], sulfobetaine methacrylate and carboxybetaine methacrylate could attract quite a lot water molecules to prevent fouling [31]. However, to grafting the polymers to a hydrophobic substrate as PVDF, selection of the chemical structure is crucial. Hydrolytic condensation of sulfobetaine siloxane can be grafted to the hydroxylated membrane via acetal reaction. Thus, a zwitterionomer, 3-[[3-(triethoxysilyl)-propyl] amino] propane-1-sulfonic acid (TPAPS) [33] was selected for this purpose and grafted onto a hydroxylated PVDF microfiltration membrane. The surface elements, lowest entry pressure (LEP), water contact angle, surface morphology and pore size distribution of the membranes were characterized in order to confirm the surface grafting and its effects on membrane characteristics. DCMD performance of the modified membrane in concentrating up to the volumetric concentration factor of 10 was evaluated and compared with the pristine PVDF membrane. Surface properties of the membrane before and after the DCMD experiments were analyzed in order to assess the anti-wetting and antifouling

performance of the surface modified membranes. Present work aims to provide an engineering method for the development of fouling resistant membranes.

## 2. Experimental

### 2.1. Chemicals and membrane materials

Commercial PVDF flat membranes were purchased from Millipore GVHP (125 μm in thickness, nominal pore size of 0.22 μm). Sodium dodecyl sulfate (SDS), (3-aminopropyl) triethoxysilane (APTEOS), tetraethoxysilane (TEOS), tetrahydrofuran (THF), and 3-propanesultone were from Sigma Aldrich Chemicals. Ethanol (AR), sodium hydroxide (NaOH) and sodium chloride (NaCl, AR), sodium bicarbonate (NaHCO<sub>3</sub>), humic acid (HA), calcium chloride (CaCl<sub>2</sub>), ammonium chloride (NH<sub>4</sub>Cl), Cellulose, Kaolin, and Casein were obtained from Sinopharm Chemical Reagent Co., Ltd. (Shanghai, China). All the chemicals were used as received. Deionized water (DI water) was used for preparing solutions in DCMD.

### 2.2. Surface modification of PVDF membrane

A two-step surface modification process is shown in Fig. 1: (1) Hydroxylation of the PVDF membrane surface; the pristine PVDF membrane (PVDF-V) was placed floating on top of the solution of NaOH (7.5 mol/L) for 1 h at 60 °C; then, the membrane was rinsed with DI water and dried in an oven at 30 °C. The modified membrane is named as PVDF-OH [34]; (2) Grafting procedure; the pre-synthesized zwitterion 3-[[3-(triethoxysilyl)-propyl]amino]propane-1-sulfonic acid (TPAPS, 5 g) was dissolved in 95 g DI water at pH = 2 together with TEOS (molar ratio is 2:1) at constant magnetic stirring for 12 h at room temperature [33]; TEOS was used as the cross-linker for the zwitterionomers (Fig. 1). The membrane after surface hydroxylation was placed on the solution surface for 1 h. Afterwards, the membrane was placed in a mixed solution (HCHO + H<sub>2</sub>SO<sub>4</sub>) for 3 h at 40 °C [33]. The resulting membrane is coded as PVDF-T.

### 2.3. Instrumental characterization

The membrane morphology was examined by a ZEISS SUPRATM 55 scanning electron microscope (SEM). Cross section samples were prepared by breaking the membrane under a cryogenic condition, and then with gold coating. To analyze the chemical change of the membrane before and after surface modification, Energy Dispersive X-Ray Spectroscopy (Oxford, X-Max Extreme) (EDS) and X-ray photoelectron spectroscopy (K-alpha, Thermo Fisher) (XPS) was utilized. Surface survey data was collected followed by high-resolution scans over S2p (154–176 eV), C1s (279–297 eV), N1s (393–411 eV), and F1s (679–699 eV). A streaming electrokinetic analyzer (Surpass Anton Paar, Austria) was used to characterize the membrane surface charges before and after the fouling test [35,36]. The zeta potential was analyzed at different pH values.

A sessile drop method was adopted to assess the membrane surface wettability using a contact angle goniometer (Maist Drop Meter A-100P) equipped with a highspeed CCD camera. The average of at least five measurements was reported [37,38]. The LEP of the membranes (for a sample of 2 cm<sup>2</sup>) was measured following our previous reported method by increase of the pressure at step of 0.02 bar in every 3 min. The pressure at the first drop of water break through was determined to be the LEP for the membranes.

### 2.4. Concentrating grey water in DCMD

The composition of a synthetic grey water (Supplementary data Table S1) was the same as published before [7]. To remove the foulants in the water and prevent instantaneous fouling, we pre-treated the

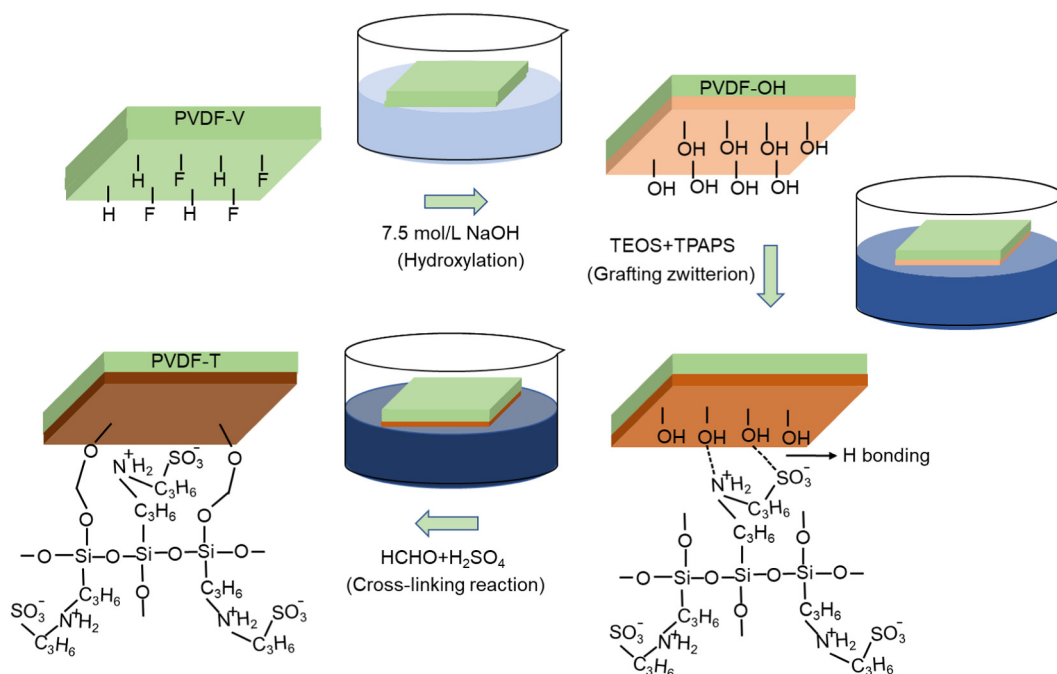


**Fig. 1.** Schematic illustration for zwitterionic grafted PVDF hydrophilic-hydrophobic composite membrane (PVDF-T) [34]. To avoid progressive surface modification, the membrane was dipped on the liquid surface for reaction. The dashed lines represent hydrogen bonding. The green color represents the original hydrophobic layer. The thickness of the surface layer is exaggerated for clear view.

**Table 1**  
Components related to fouling and permeate quality after flocculation.

Analytes	Concentration (mg/L)
Ca <sup>2+</sup>	10.9 ± 0.1
NH <sub>4</sub> <sup>+</sup>	2.2 ± 0.1
PO <sub>3</sub> <sup>-</sup>	2.0 ± 0.1
Humic acid	7.1 ± 0.7
SDS	12.2 ± 0.8
Casein	33.2 ± 2.1
Conductivity (μs/cm)	1560.0 ± 100.0
pH	6.9 ± 0.2

greywater by flocculation using FeCl<sub>3</sub> (70 mg/L) [7,39]. After flocculation, the precipitate was filtered using a disc filter paper (45 μm). The constituents related to the fouling in the flocculated and filtered water are listed in Table 1. The photos of the synthetic greywater and the water after pre-treatment are shown in Fig. S1 (Supplementary data). Rather clear water was obtained via flocculation from a highly suspended brownish greywater. The clean pre-treated water was used as the feed solution in DCMD to evaluate the membrane performance.

The fouling behaviors of the membranes were studied using a DCMD setup as described in our previous works [20,37]. Both feed and permeate temperature were maintained constant at 60.0 ± 0.3 °C and 20.0 ± 0.3 °C, respectively. The velocity of the feed and permeate was 0.11 m/s. The MD process was continued as a concentrating process and a concentration factor was defined as the ratio of V<sub>0</sub>/V<sub>t</sub>, where V<sub>0</sub> and V<sub>t</sub> representing the initial volume and that at a processing time of *t*. The water flux (J, kg/m<sup>2</sup>·h) was determined by tracking the weight of water transported from feed to permeate (Δ*m*, kg) per unit membrane area (A = 0.003 m<sup>2</sup> in this experiment) and time (Δ*t*, h) as

$$J = \frac{\Delta m}{A \Delta t} \quad (1)$$

Most of the literature reported salt rejection of DCMD was based on the salt concentration in the permeate and the feed. In this approach, the permeate salt concentration reflects the final mixture of the water

permeate through the membrane and the initial permeate volume in the permeate tank. In case the total permeate volume is small comparing to the initial volume, this calculation is not a real measure of the membrane rejection in DCMD. Thus, we calculated the salt rejection (R) based on the salt concentration in the water permeated across the membrane divided by the feed concentration as [40].

$$R = \left( 1 - \frac{V_p C_p}{J A \Delta t C_f} \right) \times 100\% \quad (2)$$

where C<sub>p</sub> and C<sub>f</sub> represent the concentration of salt in the permeate and the feed, respectively. Electric conductivity of the permeate solution was monitored by the conductivity sensor (EC-4300RS, SUNTXE Instrument Ltd.) to determine the salt concentration based on a concentration vs conductivity calibration curve. V<sub>p</sub> is the volume of permeate added to the original solution at the permeate side.

### 3. Results and discussion

#### 3.1. Characteristics of the membranes

The top surface morphologies of the virgin and surface modified PVDF membranes are shown in Fig. 2. Larger leafy-like polymeric aggregates are observed on the PVDF-V surface, but smaller protuberance aggregates are found in the PVDF-T surface as indicated by some nanosized particles were observed on the large PVDF threads (Fig. 2 PVDF-T). The EDS analysis was used to identify the chemical content of the top surface of the PVDF membrane. As shown in Fig. 2, the N, O and S elements in the top surface of the PVDF-T membrane confirm the successful grafting of the TPAPS.

Shown in the inset of Fig. 2 are the images of a water droplet sitting on top of the membrane surface for static water contact angle measurements. Clearly the membrane has transformed from a rather hydrophobic surface (131°) to a hydrophilic one (75°). The PVDF-OH membrane showed a contact angle of about 70° ± 9° (Table 2), due to replacement of F atom by the OH groups during the hydroxylation process using concentrated NaOH solution [35,36]. We noticed that the

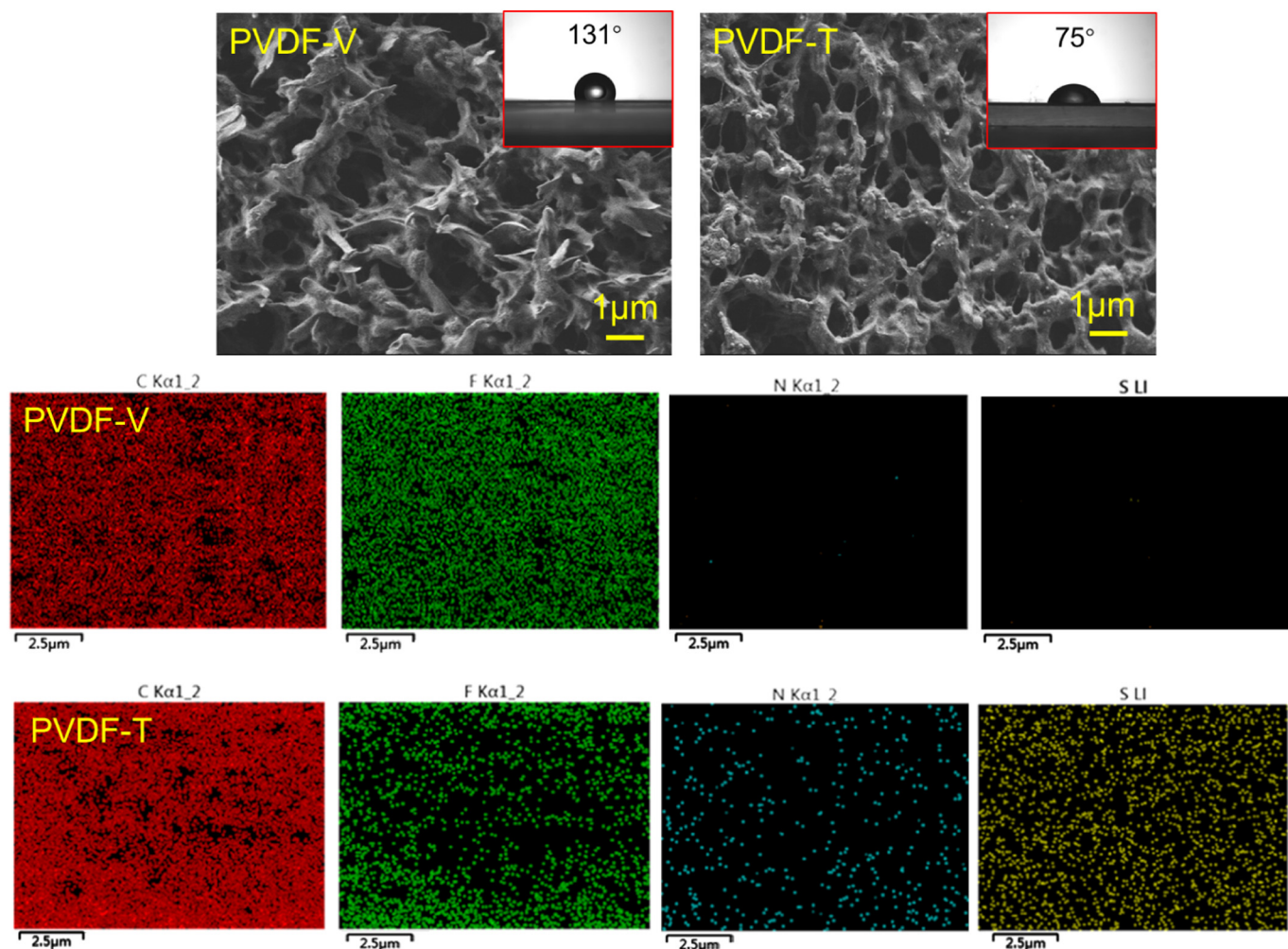


Fig. 2. (Above) SEM images of the top surface morphologies and contact angles of the PVDF-V and PVDF-T membranes; (Bottom) EDS mapping of the top surface of the PVDF-V and PVDF-T.

surface morphology of PVDF-OH membrane was similar to the PVDF-V (Supplementary data Fig. S3); but slightly more open surface pores were identified. In order to improve significantly the hydrophilicity of the PVDF membranes for high density of hydroxylation groups, highly concentrated caustic solution was utilized (referring to Fig. 1). This might result in minor partial surface damage and slightly more open top surface. The consequence of the change in transport properties will be addressed later (referring to Table 2). Slightly higher value in the contact angle of PVDF-T membrane also confirmed that the PVDF-OH was grafted with zwitterionic TPAPS since hydroxyl groups tend to form hydrogen bonds with water molecules, thus the membrane surface is more hydrophilic. Table 2 shows that the contact angle of the bottom surface was basically unchanged.

In order to confirm the surface grafting, XPS analyses were carried out on the membrane surfaces. The survey scans of the top surface of the PVDF-V and PVDF-T membrane are presented in Fig. 3. The appearance of the N 1s and S 2p peaks along with the appearance of Si 2p peak on the top surface of the PVDF-T membrane suggested the

successfully grafted of TPAPS on membrane surface, which is in agreement with the water contact angle change. As shown in the survey scans of the PVDF membranes in Fig. 3a and b, the C 1s core-level spectrum could be curve-fitted with the peak component at binding energy of 287.8 eV, which corresponded to the C–C bonds. In Fig. 3b, peak in the region of 398.4 eV indicated the presence of quaternary ammonium groups. The presence of a sulfonic acid group in the membrane matrix was confirmed because of the binding energy present at 168.5 eV. The Si 2p core level spectrum was curve-fitted with the peak components at binding energy of 102.6 eV, which were assigned to the Si–O bonds groups. It is clear that Si–O groups are the result of a condensation reaction between the Si–OH group from a hydrolyzed zwitterionomer and TEOS and C–OH groups from PVDF. The XPS analysis results are supportive of the TPAPS grafting to the PVDF membrane.

Liquid entry pressure is an important indicator of the membrane ability against wetting. Present results show that the PVDF-T membrane has a slightly lower LEP value than that of the PVDF-V membrane

Table 2

Contact angle (CA), permeability, mean flow size and LEP of the membranes.

	CA of top surface (°)	CA of bottom surface (°)	Nitrogen flux (L/min/cm <sup>2</sup> )	Mean flow pore size (μm)	LEP (MPa)
PVDF-V	131 ± 5	123 ± 2	0.070 ± 0.001	0.220 ± 0.001	0.221 ± 0.002
PVDF-OH	70 ± 9	121 ± 6	0.073 ± 0.005	0.221 ± 0.001	0.215 ± 0.002
PVDF-T	75 ± 5	121 ± 9	0.040 ± 0.005	0.184 ± 0.010	0.216 ± 0.002

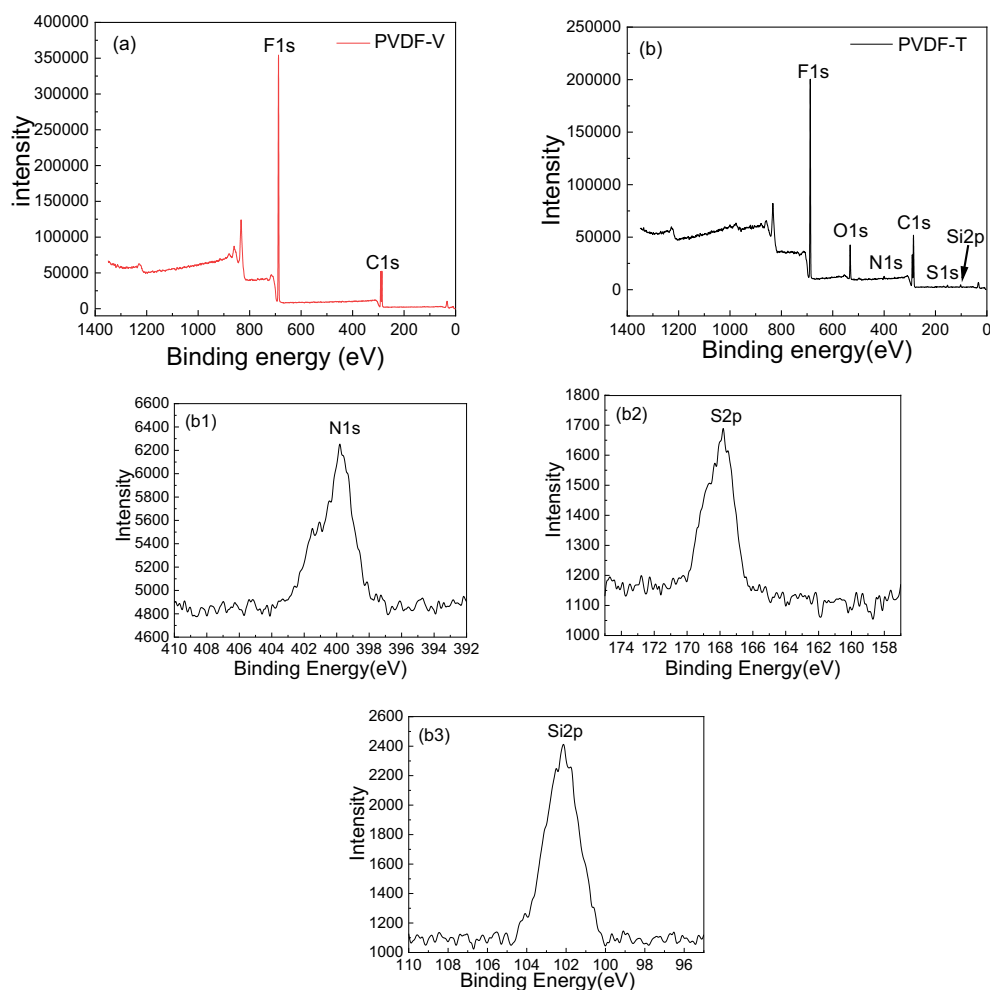


Fig. 3. XPS survey scans of the top surface of (a) PVDF-V and (b) PVDF-T membranes. Deconvolution of (b1) N 1s, (b2) S 2p and Si 2p spectra of the top surface of the PVDF-T membrane.

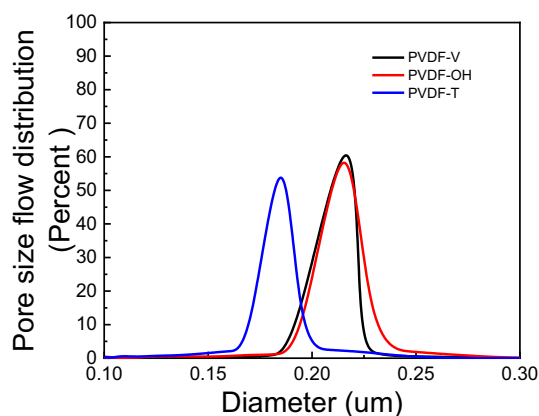


Fig. 4. Pore size distribution of PVDF-V, PVDF-OH and PVDF-T membranes.

(Table 2). This is understood as that the hydrophilic grafting only takes place at the surface and the bulk of the membrane remained hydrophobic. Decreased LEP means that increase in maximal pore size, or the surface pores are slightly smaller than those beneath this surface layer. To further characterize the PVDF-T membrane, a “dry” test using gas permeation was used to show the impact of the zwitterionic coating. As listed in Table 2, the nitrogen flux of the PVDF-V and PVDF-OH membranes are very similar about  $0.070 \text{ L/min/cm}^2$ , but for PVDF-T membrane, the flux was reduced to  $0.040 \text{ L/min/cm}^2$ , a reduction of

43%; this corresponds to the reduction in the mean flow pore size from  $0.220 \mu\text{m}$  to  $0.184 \mu\text{m}$ , as shown in Fig. 4. It is difficult to discern an obvious reduction in the surface pore size from the SEM images as shown in Fig. 2, but the grafting of zwitterionic TPAPS certainly had strongly influenced on the mean flow pore size (Fig. 4).

### 3.2. DCMD performance

The DCMD flux and rejection of PVDF-V and PVDF-T membranes are shown in Fig. 5a using  $40 \text{ g/L}$  NaCl solution as feed. A slightly higher flux was observed for the PVDF-T ( $22.6 \text{ kg/m}^2\text{h}$ ) than the PVDF-V ( $20.3 \text{ kg/m}^2\text{h}$ ). Within 60 min, both membranes appeared to show stable performance in terms flux and permeate conductivity, thus no observed salt leakage. This is rather interesting and confirmed that the hydrophilic zwitterionic surface grafting did not alter the hydrophobic nature of the PVDF-T, which agrees to the LEP results. The increased flux of the PVDF-T membrane is not expected according to the gas flow test where an increased mass transfer was observed. However, we believe another scenario may take place as follows. The PVDF-T membrane has a hydrophilic top layer, which means the feed water can penetration to a deeper depth from the membrane surface. In essence, the air water interface has been pushed forward into the membrane pores where the new hydrophobic/hydrophilic interfaces are generated, and thus the actual hydrophobic layer is slightly thinner than the unmodified PVDF-V membrane; consequently, the mass transfer resistance of the PVDF-T membrane is reduced, resulting in increased

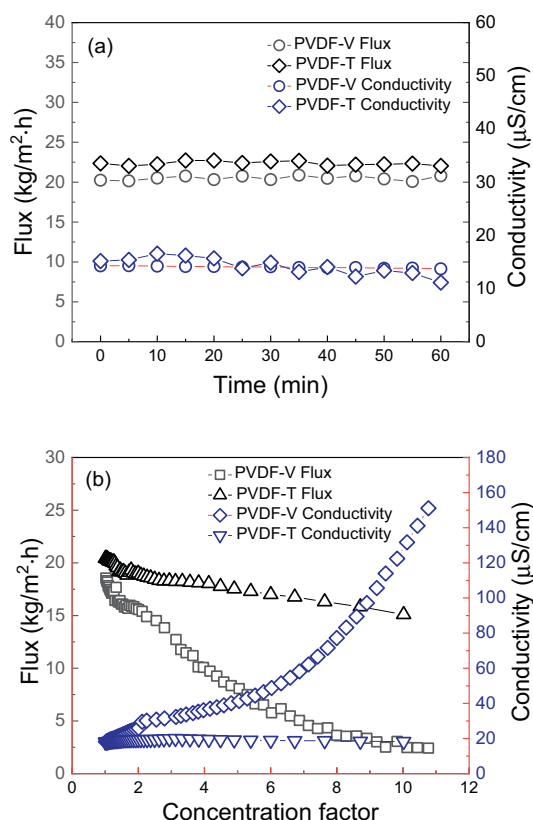


**Fig. 5.** (a) Flux and conductivity profiles for PVDF-V and PVDF-T membranes using 40 g/L NaCl solution as feed; (b) Flux and conductivity profiles for PVDF-V and PVDF-T membranes using flocculated grey water as feed solutions; (operating conditions of (a) (b): Feed:  $60.0 \pm 0.5$  °C; Permeate: DI water,  $20.0 \pm 0.5$  °C); The velocity for the feed and permeate was 0.11 m/s.

flux.

When using pre-treated greywater as the feed, the initial DCMD flux of the PVDF-T membrane ( $20.4 \text{ kg/m}^2\cdot\text{h}$ ) was also higher than the PVDF-V membrane ( $18.5 \text{ kg/m}^2\cdot\text{h}$ ) (Fig. 5b). This might be due to the more severe initial fouling in PVDF-V membrane during the startup stage of the MD process. Gradual flux decreases were observed for both PVDF-T and PVDF-V as the concentration factor increased. As the concentration process proceeded, the salinity in the feed increases; thus, a concentration factor of 10 (the salinity increases 10 times) resulted in a reduced vapor pressure and flux. For the PVDF-T membrane, the end flux was about  $15.1 \text{ kg/m}^2\cdot\text{h}$ , but for PVDF-V membrane, the flux dropped sharply down to  $2.4 \text{ kg/m}^2\cdot\text{h}$ , which is much lower than the initial flux of  $18.5 \text{ kg/m}^2\cdot\text{h}$ .

Because the initial feed contains equivalent molar concentration to NaCl about 13 mmol/L (Table S1), the final salinity is 130 mmol/L, which is about 1/5 of the initial NaCl concentration used in Fig. 5a ( $40 \text{ g/L} \sim 684 \text{ mmol/L}$ ). Comparing to the initial flux in Fig. 5a, the significantly low flux of PVDF-V membrane ( $2.4 \text{ kg/m}^2\cdot\text{h}$ ) at concentration factor of 10 indicates that a severe membrane fouling occurred; the flux of PVDF-T membrane ( $15.1 \text{ kg/m}^2\cdot\text{h}$ ) is also lower than the initial MD flux in Fig. 5a ( $22.6 \text{ kg/m}^2\cdot\text{h}$ ), but the fouling rate has been at a much slower pace than PVDF-V membrane. This result indeed shows that the zwitterionic grafted hydrophilic-hydrophobic membrane showed much better fouling resistance than the hydrophobic PVDF-V membrane.

In contrast, the MD flux of PVDF-V membrane and the permeate conductivity shoot up to  $151 \mu\text{S/cm}$  (Fig. 5b). However, the conductivity of the permeate side using PVDF-T membrane remained constant with a rejection above 99.9% (Eq. (2)). The increase of

conductivity for the PVDF-V membrane is a strong evidence of salt leakage, which was mostly caused by fouling and subsequent wetting. A qualitative analysis of the constituents in the concentrate after concentrating 10 times would justify this conclusion. By assuming 100% rejection in MD process, at a concentration factor of 10, the SDS ( $\sim 120 \text{ mg/L}$ ) and humic acid ( $\sim 70 \text{ mg/L}$ ) concentration would be significantly higher than before flocculation; for casein ( $\sim 330 \text{ mg/L}$ ), the concentration is close to original value. Additionally, the concentrations of both  $\text{Ca}^{2+}$  and  $\text{PO}_4^{3-}$  are also higher than the original values. Therefore, the reduced MD flux and increased permeate conductivity for PVDF-V membrane is not a surprise. In contrast, the PVDF-T membrane has demonstrated significantly improved fouling and wetting resistance. Repeated experimental results (Supplementary data Figs. S4 and S5) showed very similar trend in the fouling resistance.

### 3.3. Membrane autopsy

After the DCMD treatment of the greywater feed, visual inspection of the PVDF-V membrane showed yellowish on the top surface in contrast to the slight surface color change (Fig. 6). Rinsing with DI water did not change the visual appearance. SEM images of PVDF-V membrane confirmed the presence of foulants at both low and high magnifications in contrast to the largely clean PVDF-T with sporadic deposition of foulants (Fig. 6 Bottom). The XPS survey scan spectra of the top surface of the PVDF-V and PVDF-T membranes after fouling test are shown in the Fig. S6 (Supplementary data). The appearance of the N 1 s peak on the top surface of the PVDF-V fouling membrane also represented the PVDF-V membrane was fouled.

Fig. 7 shows the zeta potential of PVDF-V and PVDF-T membranes before and after experiment. Both of PVDF-V and PVDF-T were negatively charged in the pH range of 4–10. Literature reports have shown that an interface of a solid hydrophobic surface adjacent to water do appear to be negatively charged due to dissociation of the water molecules at the interface [41–43]. This explains that hydrophobic PVDF membrane surface actually is strongly negatively charged. After surface grafting, the PVDF-T membrane showed more negative charges than PVDF-V due to the strongly dissociated negative charges in the zwitterionic chemicals. The same trend was reported for zwitterionic surface coated hydrophilic membranes [44]. After the fouling test, the zeta potential of both PVDF-V and the PVDF-T membranes became less negative. However, the fouled PVDF-V membrane showed a significant increase in the zeta potential at pH neutral, but the fouled PVDF-T membrane showed very similar zeta potential as the pristine one. At pH above 7, both PVDF-OH and PVDF-T membranes showed further decrease in the zeta potential (to more negative values); but the zeta potential for the fouled membranes appeared to be stabilized. Stabilized zeta potential values indicate that no extra negative charges aggregate to the surface after fouling experiment. From Fig. 6, we deduce that the characteristics is related to the foulants (mixture of HA, casein and SDS) at the membrane surface. Thus, although minor, PVDF-T membrane did also show slight fouling during concentration experiment of greywater. Further cleaning test is required for understanding robustness of the zwitterionomer grafted PVDF-T membrane. The difference is a strong support that a high negative surface potential contributes positively to the high anti-fouling properties, therefore is worthy of more in-depth exploration.

## 4. Conclusions

Grey water is a challenging waste stream with a fouling and wetting propensity for hydrophobic distillation membranes due to the surfactant, proteins and organic contaminants. In this paper, the zwitterionic surface grafting was introduced onto the surface to improve the fouling resistance of the PVDF membrane in concentrating the greywater. Hydroxylation followed by grafting TPAPS resulted in a composite structure consisting of a hydrophilic top surface and a hydrophobic

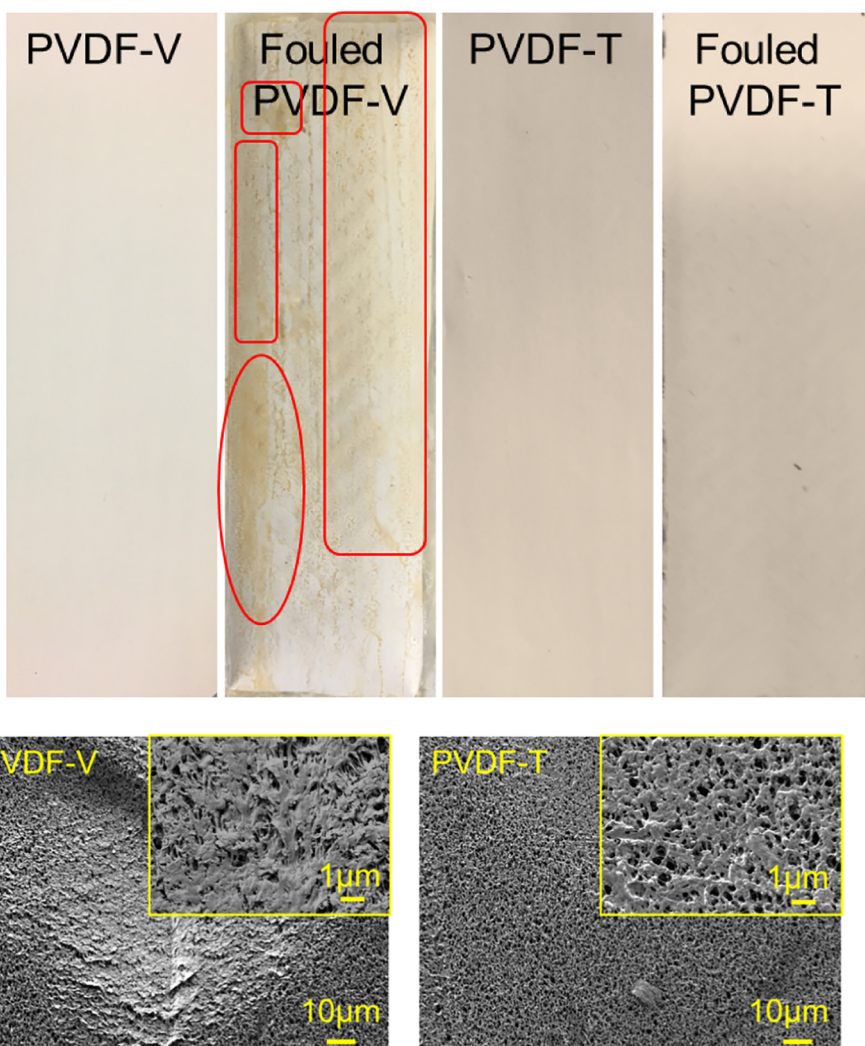


Fig. 6. (Top) Photographs of the PVDF-V and PVDF-T membranes before and after MD test using greywater as the feed. (Bottom) SEM images of the top surface morphologies of PVDF-V and PVDF-T membranes after treating grey water in DCMD.

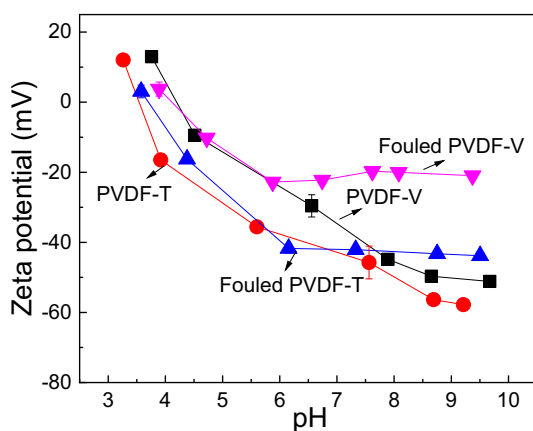


Fig. 7. Zeta potential of the PVDF-V and PVDF-T membranes before and after testing using grey water.

support. Additional mass transfer resistance was identified by gas flux measurement, corresponding to reduced pore size. Slightly reduced LEP value after surface modification indicated larger pores beneath the surface. Similar DCMD flux was obtained when treating a 4 wt% NaCl solution without salt leakage. Upon concentrating flocculated

greywater, the TPAPS grafted PVDF membrane showed much less flux decline than the pristine PVDF membrane without any increase in permeate conductivity. After fouling test, the surface characterization proved that the TPAPS modified PVDF membrane was less accessible to the organic fouling in the greywater. The improved fouling resistance was ascribed to the surface hydrophilicity and charge effect due to the chemical grafting with zwitterions. This work provides new directions for the development of antifouling MD membranes for treating lightly contaminated waste streams containing proteins, surfactants and other organic foulants.

**Acknowledgments**

This study was partially supported by National Natural Science Foundation of China (Project No. U1507117, 21676290, 51861145313, 21808236). We appreciate the financial support from Newton Advanced Fellowships (No. NA170113).

**Appendix A. Supplementary data**

Supplementary data to this article can be found online at <https://doi.org/10.1016/j.desal.2019.01.009>.

## References

- [1] M. Elimelech, W.A. Phillip, The future of seawater desalination: energy, technology, and the environment, *Science* 333 (2011) 712.
- [2] H. Buisson, P. Cote, M. Praderie, H. Paillard, The use of immersed membranes for upgrading wastewater treatment plants, *Water Sci. Technol.* 37 (1998) 89–95.
- [3] L.A. Ghunmi, G. Zeeman, M. Fayyad, J.B. van Lier, Grey water treatment systems: a review, *Crit. Rev. Environ. Sci. Technol.* 41 (2011) 657–698.
- [4] E. Eriksson, K. Auffarth, M. Henze, A. Ledin, Characteristics of grey wastewater, *Urban Water J.* 4 (2002) 85–104.
- [5] R. Otterpohl, A. Albold, M. Oldenburg, Source control in urban sanitation and waste management: ten systems with reuse of resources, *Water Sci. Technol.* 39 (1999) 153–160.
- [6] M. Gryta, Fouling in direct contact membrane distillation process, *J. Membr. Sci.* 325 (2008) 383–394.
- [7] T. Xiao, P. Dou, J. Wang, J. Song, Y. Wang, X.-M. Li, T. He, Concentrating greywater using hollow fiber thin film composite forward osmosis membranes: fouling and process optimization, *Chem. Eng. Sci.* 190 (2018) 140–148.
- [8] S. Pellicer, G. Santa, A.L. Bleda, R. Maestre, A.J. Jara, A. Gomez Skarmeta, A Global Perspective of Smart Cities: A Survey, (2013).
- [9] I. Zubizarreta, A. Seravalli, S. Arrizabalaga, Smart City concept: what it is and what it should be, *J. Urban Plann. Dev.* 142 (2016).
- [10] S. Adham, A. Hussain, J.M. Matar, R. Dores, A. Janson, Application of membrane distillation for desalting brines from thermal desalination plants, *Desalination* 314 (2013) 101–108.
- [11] A. Alkudhri, N. Darwish, N. Hilal, Membrane distillation: a comprehensive review, *Desalination* 287 (2012) 2–18.
- [12] M. Gryta, M. Tomaszewska, K. Karakulski, Wastewater treatment by membrane distillation, *Desalination* 198 (2006) 67–73.
- [13] F. He, J. Gilron, H. Lee, L. Song, K.K. Sirkar, Potential for scaling by sparingly soluble salts in crossflow DCMD, *J. Membr. Sci.* 311 (2008) 68–80.
- [14] S. Hong, M. Elimelech, Chemical and physical aspects of natural organic matter (NOM) fouling of nanofiltration membranes, *J. Membr. Sci.* 132 (1997) 159–181.
- [15] G. Brans, C.G.P.H. Schroën, R.G.M. van der Sman, R.M. Boom, Membrane fractionation of milk: state of the art and challenges, *J. Membr. Sci.* 243 (2004) 263–272.
- [16] L.D. Tijing, Y.C. Woo, J.-S. Choi, S. Lee, S.-H. Kim, H.K. Shon, Fouling and its control in membrane distillation—a review, *J. Membr. Sci.* 475 (2015) 215–244.
- [17] S. Lin, S. Nejati, C. Boo, Y. Hu, C.O. Osuji, M. Elimelech, Omniphobic membrane for robust membrane distillation, *Environ. Sci. Technol. Lett.* 1 (2014) 443–447.
- [18] Y. Liao, C.H. Loh, R. Wang, A.G. Fane, Electrospun superhydrophobic membranes with unique structures for membrane distillation, *ACS Appl. Mater. Interfaces* 6 (2014) 16035–16048.
- [19] Y.-X. Huang, Z. Wang, J. Jin, J. Jin, S. Lin, Novel Janus membrane for membrane distillation with simultaneous fouling and wetting resistance, *Environ. Sci. Technol.* 51 (2017) 13304–13310.
- [20] C. Yang, X.-M. Li, J. Gilron, D.-f. Kong, Y. Yin, Y. Oren, C. Linder, T. He, CF4 plasma-modified superhydrophobic PVDF membranes for direct contact membrane distillation, *J. Membr. Sci.* 456 (2014) 155–161.
- [21] Y.-X. Huang, Z. Wang, D. Hou, S. Lin, Coaxially electrospun super-amphiphobic silica-based membrane for anti-surfactant-wetting membrane distillation, *J. Membr. Sci.* 531 (2017) 122–128.
- [22] J. Lee, C. Boo, W.-H. Ryu, A.D. Taylor, M. Elimelech, Development of omniphobic desalination membranes using a charged electrospun nanofiber scaffold, *ACS Appl. Mater. Interfaces* 8 (2016) 11154–11161.
- [23] Z. Wang, S. Lin, Membrane fouling and wetting in membrane distillation and their mitigation by novel membranes with special wettability, *Water Res.* 112 (2017) 38–47.
- [24] Z. Wang, D. Hou, S. Lin, Composite membrane with underwater-oleophobic surface for anti-oil-fouling membrane distillation, *Environ. Sci. Technol.* 50 (2016) 3866–3874.
- [25] G. Zuo, R. Wang, Novel membrane surface modification to enhance anti-oil fouling property for membrane distillation application, *J. Membr. Sci.* 447 (2013) 26–35.
- [26] H.-C. Yang, W. Zhong, J. Hou, V. Chen, Z.-K. Xu, Janus hollow fiber membrane with a mussel-inspired coating on the lumen surface for direct contact membrane distillation, *J. Membr. Sci.* 523 (2017) 1–7.
- [27] M. He, K. Gao, L. Zhou, Z. Jiao, M. Wu, J. Cao, X. You, Z. Cai, Y. Su, Z. Jiang, Zwitterionic materials for antifouling membrane surface construction, *Acta Biomater.* 40 (2016) 142–152.
- [28] C. Liu, J. Lee, C. Small, J. Ma, M. Elimelech, Comparison of organic fouling resistance of thin-film composite membranes modified by hydrophilic silica nanoparticles and zwitterionic polymer brushes, *J. Membr. Sci.* 544 (2017) 135–142.
- [29] S.-Y. Wang, L.-F. Fang, L. Cheng, S. Jeon, N. Kato, H. Matsuyama, Improved antifouling properties of membranes by simple introduction of zwitterionic copolymers via electrostatic adsorption, *J. Membr. Sci.* 564 (2018) 672–681.
- [30] J. Wang, T. Xiao, R. Bao, T. Li, Y. Wang, D. Li, X. Li, T. He, Zwitterionic surface modification of forward osmosis membranes using N-aminoethyl piperazine propane sulfonate for grey water treatment, *Process. Saf. Environ. Prot.* 116 (2018) 632–639.
- [31] Q. Shao, Y. He, A.D. White, S. Jiang, Difference in hydration between carboxybetaine and sulfobetaine, *J. Phys. Chem. B* 114 (2010) 16625–16631.
- [32] J.B. Schlenoff, Zwitteration: coating surfaces with zwitterionic functionality to reduce nonspecific adsorption, *Langmuir* 30 (2014) 9625–9636.
- [33] B.P. Tripathi, V.K. Shahi, 3-[[3-(Triethoxysilyl)propyl]amino]propane-1-sulfonic acid-poly(vinyl alcohol) cross-linked zwitterionic polymer electrolyte membranes for direct methanol fuel cell applications, *ACS Appl. Mater. Interfaces* 1 (2009) 1002–1012.
- [34] R. Zangi, J.B.F.N. Engberts, Physisorption of hydroxide ions from aqueous solution to a hydrophobic surface, *J. Am. Chem. Soc.* 127 (2005) 2272–2276.
- [35] R. Zheng, Y. Chen, J. Wang, J. Song, X.-M. Li, T. He, Preparation of omniphobic PVDF membrane with hierarchical structure for treating saline oily wastewater using direct contact membrane distillation, *J. Membr. Sci.* 555 (2018) 197–205.
- [36] Y. Chen, M.M. Tian, X.M. Li, Y.Q. Wang, A.K. An, J.H. Fang, T. He, Anti-wetting behavior of negatively charged superhydrophobic PVDF membranes in direct contact membrane distillation of emulsified wastewaters, *J. Membr. Sci.* 535 (2017) 230–238.
- [37] M. Tian, Y. Yin, C. Yang, B. Zhao, J. Song, J. Liu, X.-M. Li, T. He, CF4 plasma modified highly interconnective porous polysulfone membranes for direct contact membrane distillation (DCMD), *Desalination* 369 (2015) 105–114.
- [38] C. Yang, M. Tian, Y. Xie, X.-M. Li, B. Zhao, T. He, J. Liu, Effective evaporation of CF4 plasma modified PVDF membranes in direct contact membrane distillation, *J. Membr. Sci.* 482 (2015) 25–32.
- [39] N. Oschmann, L.D. Nghiem, A.I. Schäfer, Fouling mechanisms of submerged ultrafiltration membranes in greywater recycling, *Desalination* 179 (2005) 215–223.
- [40] L.A. Hoover, W.A. Phillip, A. Tiraferri, N.Y. Yip, M. Elimelech, Forward with osmosis: emerging applications for greater sustainability, *Environ. Sci. Technol.* 45 (2011) 9824–9830.
- [41] R. Zimmermann, S. Dukhin, C. Werner, Electrokinetic measurements reveal interfacial charge at polymer films caused by simple electrolyte ions, *J. Phys. Chem. B* 105 (2001) 8544–8549.
- [42] J.K. Beattie, The intrinsic charge on hydrophobic microfluidic substrates, *Lab Chip* 6 (2006) 1409.
- [43] B.D. Coday, T. Luxbacher, A.E. Childress, N. Almaraz, P. Xu, T.Y. Cath, Indirect determination of zeta potential at high ionic strength: specific application to semipermeable polymeric membranes, *J. Membr. Sci.* 478 (2015) 58–64.
- [44] L.-J. Zhu, F. Liu, X.-M. Yu, A.-L. Gao, L.-X. Xue, Surface zwitterionization of hemocompatible poly(lactic acid) membranes for hemodiafiltration, *J. Membr. Sci.* 475 (2015) 469–479.